PCCP

Accepted Manuscript

ROYAL SOCIETY OF CHEMISTRY

www.rsc.org/pccp

Drawing dependent structures, mechanical properties and cyclization behaviors of polyacrylonitrile and polyacrylonitrile/carbon nanotube composite fibers prepared by plasticized spinning

Xiang Li, Aiwen Qin, Xinzhen Zhao, Dapeng Liu, Haiye Wang, Chunju He*
State Key Lab for Modification of Chemical Fibers and Polymer Materials
College of Material Science & Engineering
Donghua University
Shanghai 201620 (P. R. China)

Abstract

Drawing to change the structural properties and cyclization behaviors of the polyacrylonitrile (PAN) chains in crystalline and amorphous regions is carried out on PAN and PAN/carbon nanotube (CNT) composite fibers. Various characterization methods including fourier transform infrared spectroscopy, differential scanning calorimeter, X-ray diffraction and thermal gravimetric analysis are used to monitor the structural evolution and cyclization behaviors of the fibers. With the increase of draw ratio during the plasticized spinning process, the structural parameters of the fibers, i.e. crystallinity and planar zigzag conformation are decreased at first, and then increased, which are associated with the heat exchange rate and oriented-crystallization rate. A possible mechanism for plasticized spinning is proposed to explain the changing trends of crystallinity and planar zigzag conformation. PAN and PAN/CNT fibers exhibit various cyclization behaviors induced by drawing, e.g., the initiation temperature for cyclization (T_i) of PAN fibers is increased with increasing draw ratio, while T_i of PAN/CNT fibers is decreased. Drawing also facilitates cyclization and lowers the percentage of β-amino nitrile for PAN/CNT fibers during the stabilization.

*Corresponding authors. Tel: +86-021-6779 2842. Fax: +86-021-6779 2855. E-mail: chunjuhe@dhu.edu.cn (C.J. He).

1. Introduction

Carbon fibers (CFs) have been widely utilized as an important reinforcement materials for large load-bearing composites due to their excellent tensile strength, the superior stiffness and the low density[1]. Currently, 90% of all commercial carbon fibers are fabricated through thermal conversion of polyacrylonitrile (PAN) precursors[2] due to their simple processing, low manufacturing cost and excellent mechanical properties[3]. Since the performances of CFs are critically dependent on excellent mechanical properties of PAN fibers[4], it is vital to improve the performances of PAN fibers. Carbon nanotubes (CNTs) have been considered as excellent reinforcement due to their exceptional mechanical properties, which significantly enhance the performances of the composite materials[5]. Consequently, a certain amount of CNTs has been employed to reinforce the PAN fibers[6,7] recently.

Since PAN degrades below its melting point due to its strong dipolar interaction[8-10], the PAN/CNT precursor fibers are generally prepared by wet spinning[11,12], gel spinning[13-15] and electrospinning[16,17], leading to structural defects, low efficiency, and solvent recovery problems. Therefore, external plasticization has been considered as an alternative method to prepare PAN/CNT fibers[18] owing to its high efficiency, low consumption of solvents and environmentally friendly. And, Ethylene carbonate (EC) has ever been utilized as a plasticizer for PAN/CNT system[19,20]. However, the mechanical properties of the resulting PAN/CNT fibers are very poor with diameter larger than 250μm due to poor plasticizing effect of EC. It is urgent to develop a new plasticizer so as to improve the structures and mechanical properties of the fibers. It is well known that the properties of the PAN/CNT fibers are critically dependent on the spinning processes[21]. And the drawing carried out on PAN/CNT

fibers during the wet spinning process has been considered as one of the most indispensable spinning processes, resulting in the reduction in structural imperfections[22] and the decrease in diameter[23] of the as-spun fiber. Meanwhile, due to the conformational changes of PAN chains from helical to planar zigzag[24,25], which lowers degree of chain scission during the stabilization stage and leads to the improvement of tensile strength of the resulting CFs[26]. In conclusion, we believe that drawing also plays a significant role in improving properties of the PAN fibers fabricated by plasticized spinning, which has not yet been systematically studied in depth. Furthermore, to the best of our knowledge, there are few reports concerning the effect of high draw ratio on cyclization behaviors of PAN and PAN/CNT fibers fabricated by plasticized spinning.

In this research, PAN/CNT fibers with improved mechanical properties were prepared via plasticized spinning, where 1-butyl-3-methylimidazolium chloride ([Bmim]Cl) was utilized as a novel plasticizer. The influence of drawing on structures, mechanical properties and cyclization behaviors of the prepared fibers induced by drawing were systematically studied. A possible mechanism for plasticized spinning was proposed to explain the changes in crystallinity and planar zigzag conformation of the fibers. Furthermore, various cyclization behaviors of PAN and PAN/CNTs fibers were analyzed as well. It is expected that this study will provide a better understanding on the structures, mechanical properties and cyclization behaviors of the fibers prepared by plasticized spinning and furnish an important application for the development of high-performance PAN and PAN/CNT fibers.

2. Experimental section

2.1 Materials

Pristine multi wall carbon nanotubes (CNTs, length:1-5μm, diameter: 10-20nm, nominal purity:97%) were purchased from Shenzhen Nanotech Port Corporation Limited. PAN powder ($M\eta=1.5\times10^4$g/mol) was synthesized in our laboratory.

2.2 Preparation of samples

In-situ synthesis method was utilized to prepare the [Bmim]Cl/CNT system. A mixture of 0.75 g CNT, 0.157 mol 1-chlorobutane and 0.143 mol N-methylimidazole in a 500 ml three-neck flask was sonicated for 30 min, then the mixture was conducted at 80 ℃ with magnetic stirring for 48 h under a nitrogen atmosphere. The reaction mixture was washed using ethyl acetate for three times, then [Bmim]Cl/CNT system was dried under vacuum at 80 ℃ to remove the volatile solvent residue. Then 94 g PAN powder was mixed with [Bmim]Cl/CNT system according to our previous study[27].

2.3 Plasticized spinning of PAN/CNT fibers

The PAN/CNT composite fibers were fabricated under standardized conditions of constant temperature (20 ℃ ±1 ℃) and humidity (20 % ±1 %) to ensure the reproducibility of the experimental results. The plasticized spinning process was conducted at a spinning speed in the range of 30-50 m/min, and the composite fibers were prepared through a self-made extruder at a temperature of 220 ℃. Then the prepared fibers were washed by deionized water to remove the remaining solvent and dried in an oven at 70 ℃ for 48 h.

2.4 Stabilization of PAN and PAN/CNT fibers

The PAN and PAN/CNT composite fibers were stabilized in an oven under a constant tension of 1.2 cN, a low temperature of 200 ℃ was employed.

2.5 Measurements

Optical microscope (59XD, Shanghai optical instrument factory, China) was utilized to observe the dispersion of CNTs in [Bmim]Cl/CNT system prepared by different methods.

Field emission scanning electron microscopy (FESEM, S-4800, HITACHI, Japan) was used to observe the cross-section of the fibers. The fibers were washed with alcohol for several times and dried in an oven, then embedded with epoxy resin followed by brittle fracture in liquid nitrogen. The surface and cross-section of the fibers were coated with gold before observation.

The Infrared spectra (IR) spectrum was recorded using a FTIR (Spectrum BX□, Perkin Elmer, US) spectrometer in the range of 400-4000cm^{-1} using KBr pellets.

Differential scanning calorimeter (Q20, TA, US) was used to determine the thermal performances of fibers under the nitrogen atmosphere, the fibers were heated to 400 °C and the heating rate was 10 °C/min.

The thermal resistant temperature was obtained by using a thermo-gravimetric analysis (TGA, Q5000IR, US) at a heating rate of 10 °C/min under the nitrogen atmosphere.

The X-ray diffraction analysis (XRD) using CuKα (λ=0.1542 nm) for PAN fibers was conducted under the X-ray diffractometer (D/Max-2550 PC, RIGAKU, Japan), the operation voltage and electricity were 30 kv and 10 mA respectively. The average crystal size (Lc) was calculated using the Scherrer equation[28]:

$$L_C = \frac{k\lambda}{\beta\cos\theta} \quad (1)$$

where K is the apparatus constant, which was taken to be 0.89; λ=0.1542 nm is the wavelength of the X-rays; β is the full width at half maximum in radians at 2θ =17°.

The crystallinity was determined from the XRD patterns of the fibers according to the

formula calculated by Hinrichsen's method[29]:

$$C\% = \frac{Ac}{Ac + Aa} \quad (2)$$

where Ac is the integral area of the crystalline region, and Aa is the integral area of the amorphous region.

Peakfit soft (v4.12) was utilized for peak fitting of XRD spectra in the range of 20°-50°.

The fiber tensile strength machine (XQ-1, Shanghai New Fiber Instrument Co., Ltd., China) was used to measure the mechanical properties of PAN fibers, and the statistical results came from 10 measurements for each sample.

3. Results and discussion

3.1 Dispersion of CNTs in [Bmim]Cl and PAN/CNT fibers

In order to solve the problem of CNTs aggregation, in-situ synthesis was employed to prepare [Bmim]Cl/CNT system with high homogeneity. Fig. 1 illustrates the optical micrographs of the [Bmim]Cl/CNT systems. Obviously, Fig. 1 a shows that CNTs are relatively uniformly dispersed in [Bmim]Cl through in-situ synthesis, while CNTs in [Bmim]Cl/CNT system (in Fig. 1 b), fabricated by mixing the [Bmim]Cl with CNTs under sonication, are aggregated into many large particles. The "cation-π" interaction[30-32] between CNTs and [Bmim]Cl accounts for disaggregation behavior of CNTs during the in-situ synthesis process, this interaction also results in highly stable [Bmim]Cl/CNT systems.

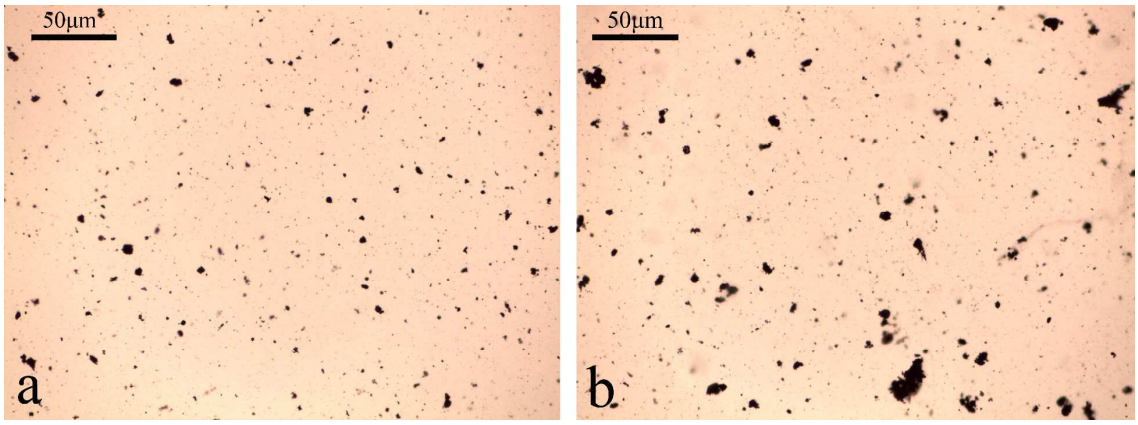

Fig. 1. Optical micrographs of the [Bmim]Cl/CNT system:(a) by in-situ synthesis; (b) by mixing.

3.2 The interaction among PAN, CNTs and [Bmim]Cl at high temperature

Fig. 2 shows FTIR spectra of [Bmim]Cl, [Bmim]Cl/CNT, PAN, PAN/[Bmim]Cl, PAN/[Bmim]Cl/CNT systems after heating at 160 ºC for 5min. 3132.2 cm^{-1} is attributed to unsaturated C-H bands of imidazolium rings in [Bmim]Cl[33,34] (in Fig. 2 a), which is blue-shifted to 3133.6 and 3135.4 cm^{-1} in P_1 (synthesis) and P_2 (mixing), respectively. The shift of these groups provides a strong evidence that there exists strong interaction between imidazolium rings in [Bmim]Cl and CNTs[31]. Obvious blue-shift of unsaturated C-H bands in P_2 reveals more CNTs are involved in the interaction, leading to better dispersion of CNTs in [Bmim]Cl.

As shown in Fig. 2 b, for PAN/[Bmim]Cl system, the red-shift of C≡N bands from 2239.5 to 2241.8 cm^{-1} and blue-shift of unsaturated C-H bands of imidazolium rings from 3132.2 to 3143.8 cm^{-1} indicates a new hydrogen bonding (C-H⋯N) has been formed between them, which has been proved in our recent work[27]. In contrast to PAN/[Bmim]Cl system, the position of C≡N groups in PAN/[Bmim]Cl/CNT is not shifted. It is well known that "π-π" interaction can be formed between CNTs and PAN, leading to red shift of C≡N groups[16]. However, the strong "cation-π" interaction between CNTs and [Bmim]Cl in PAN/[Bmim]Cl

system, as confirmed by blue shift of C-H groups of imidazolium rings from 3143.8 to 3146.1 cm^{-1} (in Fig. 2 b), leads to the weakness in interaction between PAN and [Bmim]Cl/CNT. Therefore, the blue shift of C≡N groups induced by "cation-π" interaction is offset by red shift caused by "π-π" interaction, thus the position of C≡N groups is not shifted.

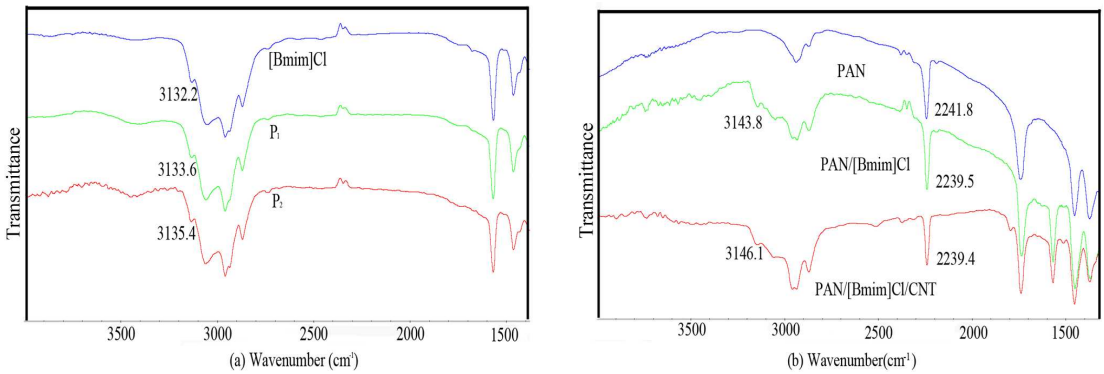

Fig. 2. IR spectra of [Bmim]Cl, [Bmim]Cl/CNT, PAN, PAN/[Bmim]Cl, PAN/[Bmim]Cl/CNT at 160 ºC temperature: P_1 ([Bmim]Cl/CNT) was prepared by in-situ synthesis process; P_2 ([Bmim]Cl/CNT) was prepared by mixing process.

3.4 The structural changes of PAN and PAN/CNT composite fibers

Fig. 3 displays the SEM images of the PAN and PAN/CNT fibers. The PAN/CNT fibers exhibit smoother surface compared with PAN fibers. The cross section of both fibers is circular and compact, and PAN/CNT fibers show a fairly uniform dispersion of apparently single CNT within the PAN matrix. This indicates that the preparation process of PAN/[Bmim]Cl/CNT system provide a better solution to problem of dispersion of CNTs in PAN matrix.

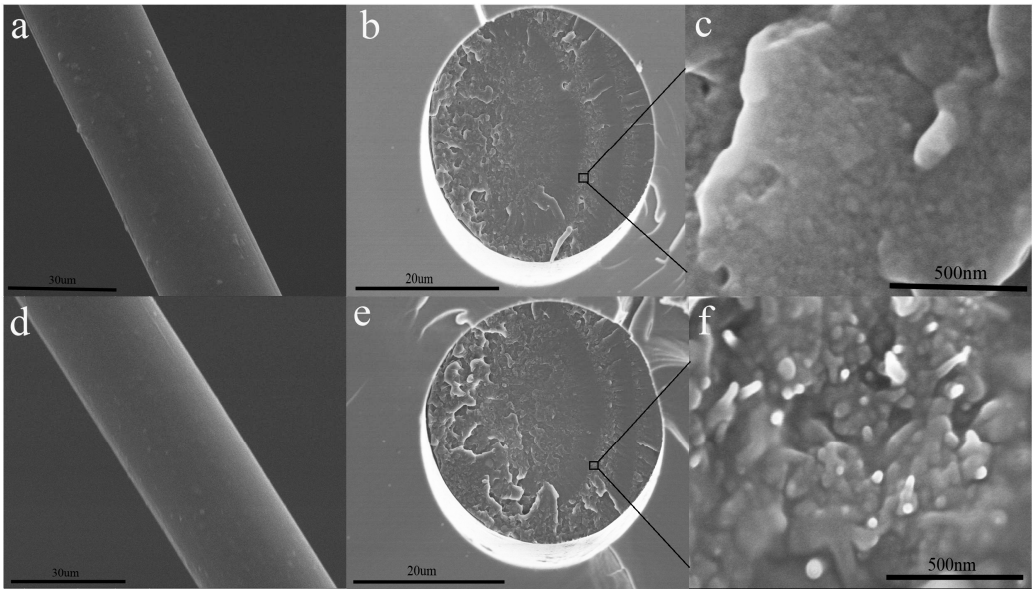

Fig. 3. SEM images of PAN and PAN/CNT fibers: (a) and (d) the surface of the fibers; (b), (c), (e) and (f) the cross section of the fibers.

As shown in Table 1, the crystallinity and planar zigzag conformation of both PAN and PAN/CNT composite fibers are first decreased with increasing draw ratio and then increased. The crystal size (1.2-1.7 nm) of PAN and PAN/CNT fibers prepared by plasticized spinning is obviously smaller than that (3.7-5 nm) of PAN and PAN/CNT fibers fabricated by wet-spinning[15], which is closely related to the difference between plasticized spinning and wet-spinning. For wet-spinning, it is suggested that[35] the slow inter-diffusion process between solvents and coagulants contributes to the growth of crystal size, the structural evolution of PAN fibers can be reasonable explained by spinodal decomposition mechanism.

Obviously, the spinodal decomposition mechanism is not suitable to explain the changing trends of structural parameters of both fibers through plasticized process, and a new possible mechanism for plasticized spinning is proposed. As shown in Fig.4, the plasticized spinning process is followed by heat exchange between PAN/[Bmim]Cl system and surrounding environment. Heat exchange rate between the thin melt and surrounding environment is so high after it's extruded from the spinneret hole, which will shorten

oriented-crystallization stage. This hinders the movement of the PAN chains and further decreases the crystallinity of the prepared fibers. On the other hand, plasticized spinning process is accompanied by oriented-crystallization of PAN molecular chains. High draw ratio contributes to orientation-crystallization of PAN chains with respect to drawing direction, leading to the increase in crystallinity of the fibers. It is concluded that drawing has two opposite effects on crystallization and changing trends in crystallinity of the resulting fibers is strongly dependent on drawing.

The changing trends in crystallinity of the composite fibers can be reasonably explained. For PAN fibers, the crystallinity of A_2 is decreased from 57.1% to 54.8% as compared with A_1. Accordingly, it is reasonable to conclude that the high heat exchange rate is the prime reason for reducing in crystallinity. As the draw ratio is further increased, it is speculated that the inter-molecular interaction becomes stronger as a result of the reduction in distance between the PAN molecular chains[27], which accelerates the extrusion rate of [Bmim]Cl from oriented-crystallization region (in Fig. 4), resulting in high oriented-crystallization rate. Although the oriented-crystallization stage is further shortened, it is believed that the high oriented-crystallization rate is a decisive factor in determining the increase in crystallinity from 54.8% to 58.6%.

For PAN/CNT composite fibers, B_1 show low crystallinity compared with A_1 (similar diameter), the similar phenomena can be observed as comparing the crystallinity between B_2 and A_2. This suggests that the addition of CNTs lowers the crystallinity of the fibers. As we know, the thermal conductivity of CNTs (2000-6000 $Wm^{-1}K^{-1}$)[36,37] is much higher than that of PAN (~0.2 $Wm^{-1}K^{-1}$)[38] and ionic liquids (0.1~0.2 $Wm^{-1}K^{-1}$)[39], which significantly

accelerates the heat exchange rate and thus reduces the oriented-crystallization stage. It is interesting to note that PAN/CNT fibers also show a similar changing trend in crystallinity compared with PAN fibers, indicating that the high oriented-crystallization rate still plays a decisive role as further increasing draw ratio. In addition, the crystallinity of A_3 is higher than that of A_1, the similar phenomena can be seen when comparing B_1 and B_3. This indicates that the oriented-crystallization rate of A_3 is significantly higher than that of A_1, through the oriented-crystallization stage of A_3 is shorter than that of A_1. The crystallinity of B_3 is increased by 1.7% compared with A_3, suggesting that the introduction of CNTs also contributes to oriented-crystallization of the PAN molecular chains during the plasticized spinning process, which accelerates the oriented-crystallization rate.

Table 1. Structural parameters of PAN and CNT/PAN composite fibers.

Fibers type	Fibers name	Draw ratio	Effective diameter /mm	Crystallinity/%	Crystal size/nm	Meridional peak position (2θ)/°
PAN	A_1	20	0.0423	57.1	1.46	40.568
	A_2	30	0.0346	54.8	1.54	40.449
	A_3	40	0.029	58.6	1.38	40.545
PAN/CNT	B_1	20	0.0434	53.6	1.44	40.398
	B_2	30	0.0352	51.8	1.32	40.252
	B_3	40	0.0305	60.3	1.63	40.373

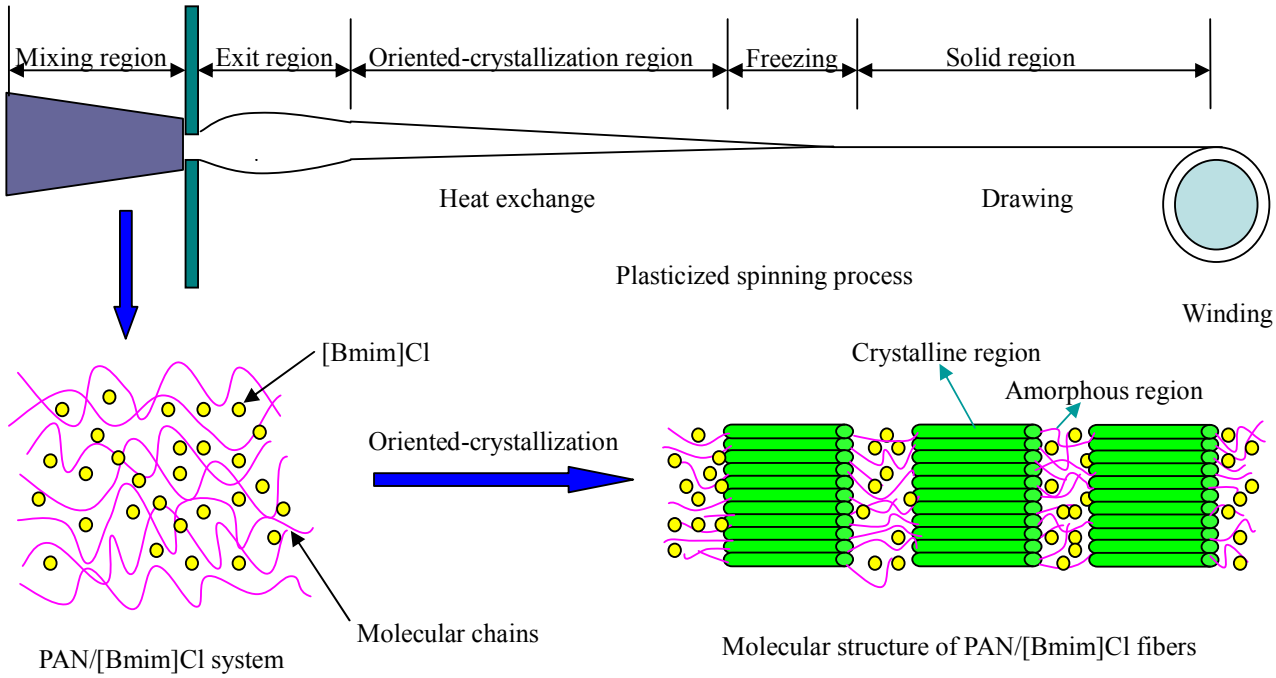

Fig. 4. The possible mechanism for plasticized spinning of PAN/[Bmim]Cl system during the plasticized spinning process.

Fig. 5 shows the XRD curves of the PAN and PAN/CNT fibers, where the peak position at around 36 and 40° are attributed to planar zigzag and helical sequences respectively[40]. The peak position at around 40° is shifted to the low angle with the increase of draw ratio, indicating the increase in planar zigzag conformation[7]. In this paper, it is interesting to note that the peak position (around 40°) of both fibers is first shifted to low angle, and then shifted to high angle with increasing draw ratio, which is consistent with the crystallinity. This reveals that the conformational changes from helical to planar zigzag are apt to take place at amorphous region rather than crystalline region, which may be due to the weak inter-molecular interaction at amorphous region[41]. Meanwhile, the PAN/CNT fibers possess more planar zigzag conformation compared with PAN fibers (similar diameter), suggesting that the introduction of the CNTs contributes to conformational changes.

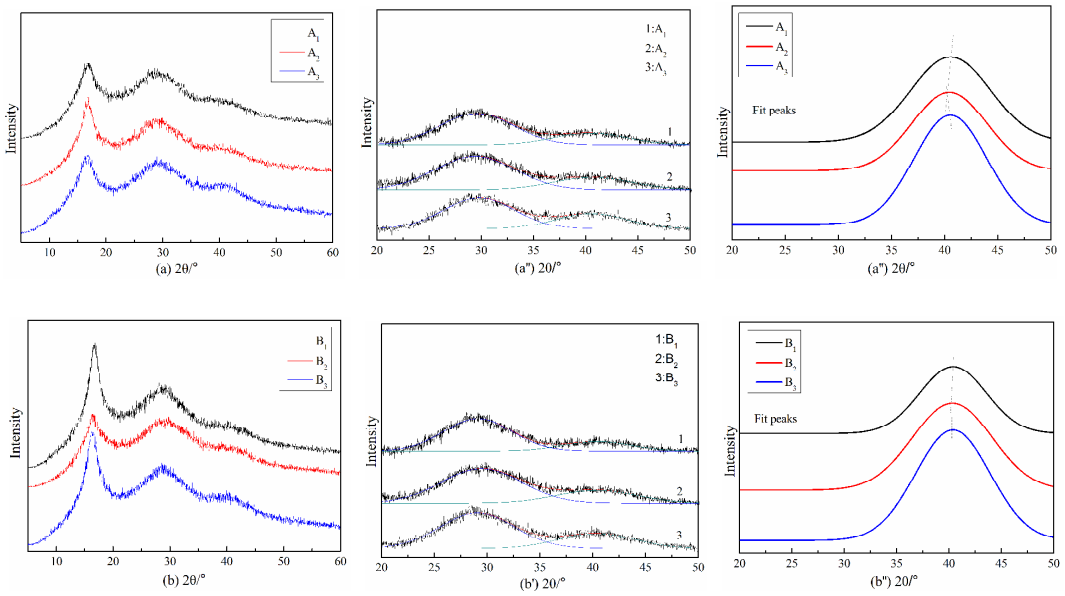

Fig. 5. XRD meridional scans: (a), (a′) and (a′′) PAN fibers; (b), (b′) and (b′′) PAN/CNT fibers;

3.4 Mechanical properties of PAN and PAN/CNT composite fibers

As can be seen in Table 2, the tensile strength and modulus of PAN/CNT fibers are as high as 0.384 GPa and 8.82 GPa even the post drawing process has not been employed, which are increased by 34.7 % and 16.7 % compared with those of PAN fibers. Meanwhile, it is noted that the tensile strength and modulus of PAN/CNT fibers are also 4.8-fold and 8.82-fold higher than those of PAN/CNT fibers prepared by EC[20]. This indicates that the plasticized effect of the [Bmim]Cl is obviously superior to EC.

The tensile strength and modulus of the both fibers are shown to gradual increase with increasing spinning speed, which are not in agreement with the changing trend of crystallinity. This suggests that the PAN molecular chains at both regions contribute to mechanical properties of the fibers prepared by plasticized spinning.

Table 2. Mechanical properties of PAN and CNT/PAN composite fibers.

Fibers type.	Fibers name	Draw ratio	Tensile strength /GPa	Tensile modulus /GPa	Strain to failure /%
PAN	A_1	20	0.19	4.49	16.02
	A_2	30	0.233	5.14	15.44
	A_3	40	0.285	7.56	13.88
PAN/CNT	B_1	20	0.227	4.5	13.12
	B_2	30	0.275	6.84	12
	B_3	40	0.384	8.82	12.36

3.5 Cyclization behaviors of the fibers characterized by DSC

Table 3 and Fig. 6 illustrate DSC data and curves of PAN and PAN/CNT composite fibers. The initiation temperature for cyclization (T_i) of PAN fibers is increased with increasing draw ratio, while T_i of PAN/CNT composite fibers is decreased. This indicates that drawing hinders the initiation of cyclization for PAN fibers, but facilitates initiation of cyclization for PAN/CNT fibers. Table 1 and Table 3 also indicate that heat released for cyclization (ΔH) of composite fibers is increased with increasing crystallinity.

Cyclization first occurs at amorphous region, then progresses to crystalline region[42,43] due to relatively loose structure of amorphous region, thus the T_i reflects the cyclization at amorphous region. The molecular chains at amorphous region are consisted of loops, folds, entanglements, chain ends, defects, co-monomer sequences, tie chains and so on[44], indicating there exists entanglement-rich region at amorphous region. The molecular chains at entanglement-rich region are apt to extend (or orient) with respect to drawing direction with increasing draw ratio[45], but the inter-molecular interaction between C≡N groups become stronger as well as a consequence of conformational changes from helical to planar zigzag[6,9], as shown in Fig. 7 a, which has been proved by XRD results. Consequently, it is reasonable to conclude that it becomes more difficult for intra-molecular cyclization[46,47] to occur, resulting in the increase in T_i for PAN fibers.

For PAN/CNT fibers, the introduction of CNTs results in formation of "π-π" interaction between PAN and CNTs (as confirmed in Fig. 2), which is beneficial to weaken inter-molecular interaction between C≡N groups at entanglement-rich region. Meanwhile, with increasing draw ratio, it is speculated that more and more C≡N groups are more likely to form the "π-π" interaction with the CNTs due to the formation of planar zigzag conformation. This further weakens the inter-molecular interaction, as shown in Fig. 7 b. The decrease in T_i of PAN/CNT composite fibers with increasing draw ratio supports the assumption.

The various cyclization behaviors can be further confirmed by heat released (ΔH) and cyclization temperature (T). The ΔH for PAN fibers is decreased from 318.9 J/g to 306.2 J/g and then increased to 324.4 J/g with increasing draw ratio, this is in agreement with changing trend of crystallinity (in Table 1), suggesting occurrence of cyclization at crystalline region mainly contributes to ΔH. The ΔH of PAN/CNT fibers is increased from 320.2 J/g to 337.3 J/g, while the crystallinity is decreased from 53.6 % to 51.8 % (in Table 1). It demonstrates that ΔH is ascribed to occurrence of cyclization both at amorphous and crystalline regions, and the "π-π" interaction and drawing facilitate the intra-molecular cyclization reaction at amorphous region.

It is believed that the cyclization temperature (T) corresponds to the occurrence of the most violent cyclization reaction at crystalline region (or both at amorphous region and crystalline region). For PAN fibers, the strong inter-molecular interaction as a result of increasing draw ratio not only hinders cyclization at amorphous region, but also obstructs the propagation of cyclization from amorphous region to crystalline region. Meanwhile, larger amorphous region is also not conducive to the occurrence of cyclization at crystalline region.

These two reasons are considered to be responsible for the increase in T from 286.4 ºC to 294.1 ºC (in Table 3). However, for PAN/CNT fibers, the T of B_2 is 285.4 ºC, which is decreased by 3.1 ºC compared with B_1 (in Table 3). This indicates that cyclization becomes easier to take place at crystalline region as a consequence of increasing drawing ratio, although the amorphous region of B_2 is larger.

Table 3. DSC data of PAN and PAN/[Bmim]Cl composite fibers in the range of 200 ºC-380 ºC.

Fibers type	Fibers name	Draw ratio	T_i/ºC	T/ºC	T_f/ºC	ΔH/Jg^{-1}
PAN	A_1	20	259.9	286.4	349.3	318.9
	A_2	30	260.6	294.1	351.8	306.2
	A_3	40	261.4	286.9	346.9	324.4
PAN/CNT	B_1	20	259.2	288.5	342	320.2
	B_2	30	257.5	285.4	351.8	337.3
	B_3	40	254.1	304.6	348.7	339.7

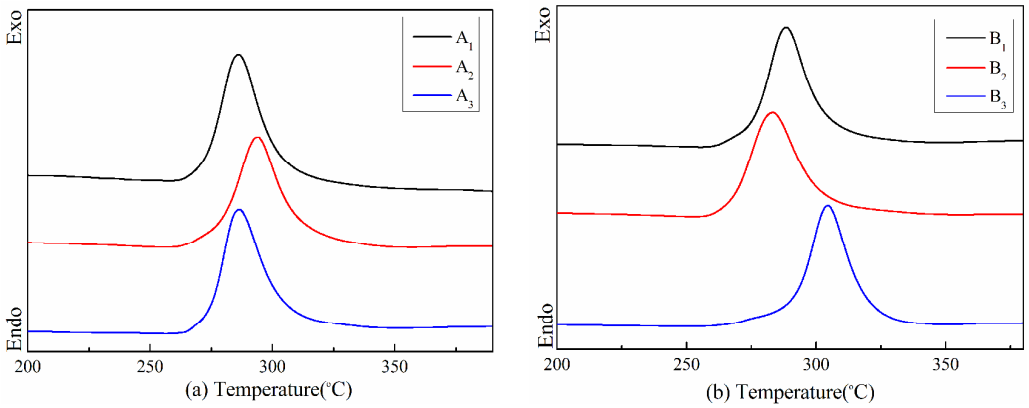

Fig. 6. DSC curves of PAN and PAN/CNT fibers: (a) PAN fibers; (b) PAN/CNT fibers.

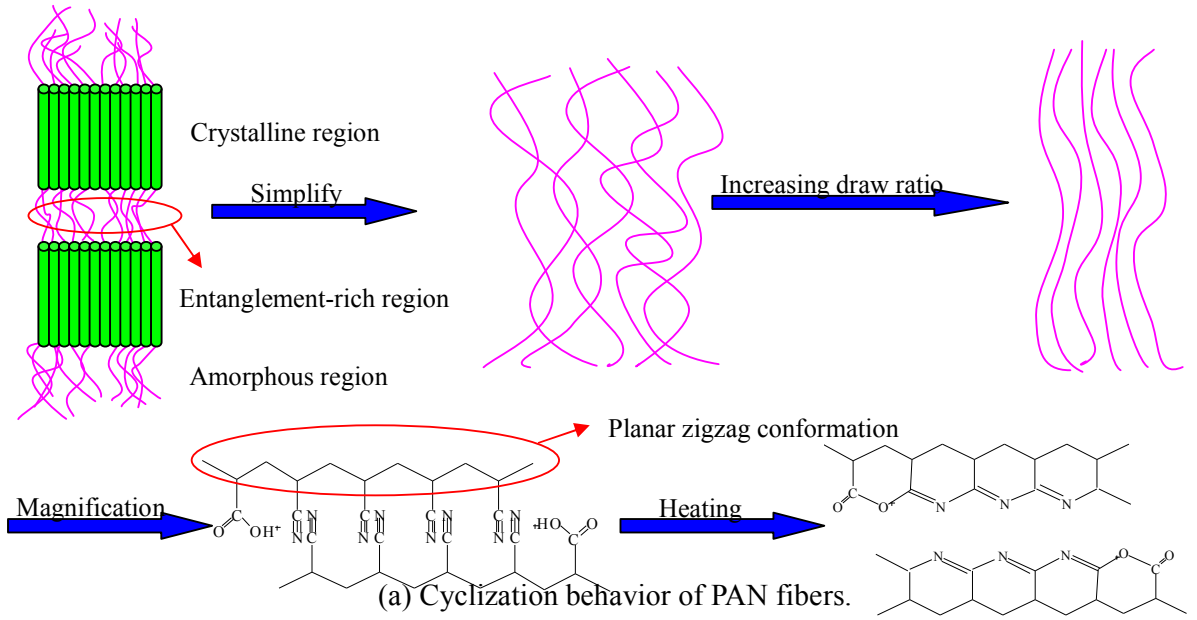

(a) Cyclization behavior of PAN fibers.

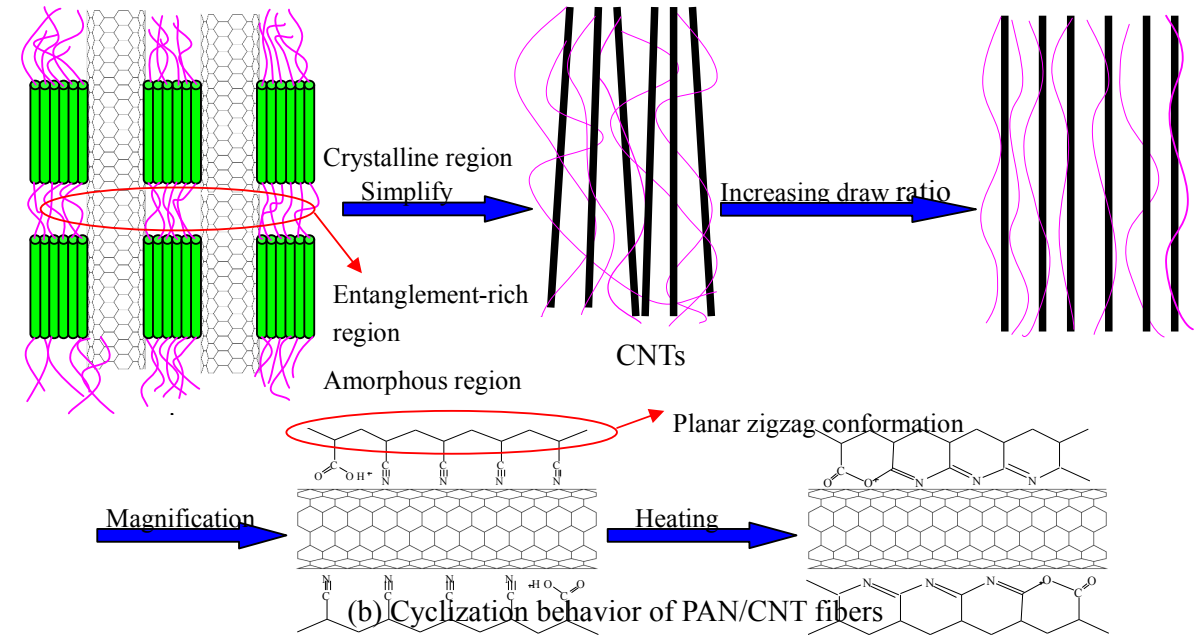

(b) Cyclization behavior of PAN/CNT fibers

Fig. 7. Cyclization behaviors of PAN and PAN/CNT composite fibers.

3.6 Cyclization behaviors of the fibers characterized by TG

Fig. 8 displays the TG curves of PAN and PAN/CNT composite fibers, where the decomposition temperature for weight loss (T_o) of PAN and PAN/CNT fibers is 256.6 ºC and 274.8 ºC, respectively. It is believed that the weakness in inter-molecular interaction, induced by CNTs, contributes to cyclization. As a result, it lowers degree of chain scission.

Fig. 8 b shows that T_o of PAN/CNT fibers is increased with increasing draw ratio. The changing trend of T_o is not in accordance with that of crystallinity (in Table 1), this confirms that decomposition first occurs at amorphous region and the increase in draw ratio lowers chain scission possibility. It is suggested that[24] the fibers contain more planar zigzag conformation result in less degree of chain scission, this further confirms that the planar zigzag conformation is increased at amorphous region with increasing draw ratio, which has been proved previously.

The changing trend of residual weight (%), which is decreased at first and then increased, is consistent with that of crystallinity (in Table 1). This indicates that molecular chains at crystalline region are not vulnerable to scission due to its regularity.

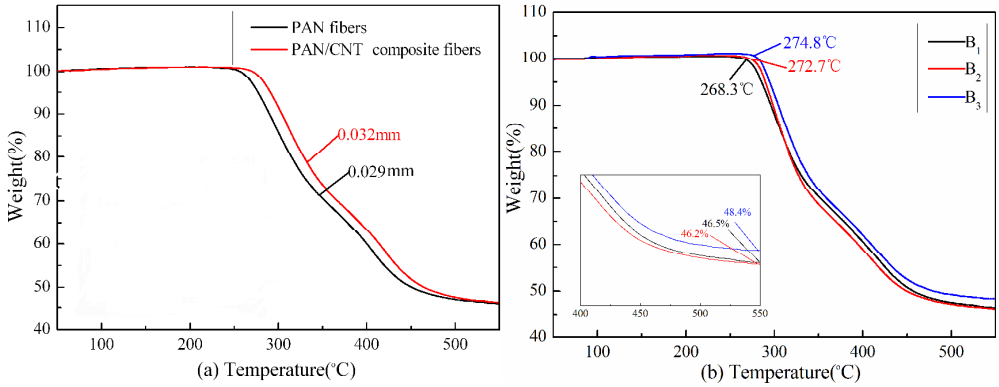

Fig. 8. TG curves of PAN and PAN/CNT composite fibers.

3.7 Cyclization behaviors of the fibers characterized by FTIR and XRD

It has been proved that the peaks in the range of 2180-2260 cm^{-1} can be ascribed to three types of C≡N groups, un-reacted nitrile at 2242 cm^{-1}, conjugated nitrile at 2210 cm^{-1} and β-amino nitrile at 2190 cm^{-1}[1,48], which can be characterized by FTIR. Meanwhile, XRD also can be used to observe the changes in crystallinity induced by stabilization[49]. Thus XRD and FTIR were utilized to characterize the stabilization of PAN and PAN/CNT composite fibers.

As can be seen in Table 4 and Fig. 9, for A_3 and B_3, the addition of CNTs lowers the percentage of β-amino nitrile in the stabilized fibers. For PAN/CNT fibers, drawing lowers the percentages of unreacted and β-amino nitrile, indicating that drawing contributes to stabilization. It is noted that a low temperature of 200 ºC was conducted to stabilize the fibers, thus the crystallinity of the composite fibers is decreased marginally (in Table 5) in the early stage (<2h), indicating cyclization mainly occurs at amorphous region. At this stage, the percentage of unreacted nitrile in B_3 is significantly lower than that in A_3, suggesting the "π-π" interaction between PAN and CNTs facilitates the intra-molecular cyclization at amorphous region.

In contrast to A_3, the quantity of unreacted nitrile in B_3 is decreased slowly as stabilization time is longer than 1h (in Table 4), and the crystallinity of B_3 is reduced slowly as well (in Table 5), confirming that the introduction of CNTs obstructs the stabilization at crystalline region.

Table 4. Peak fitting for FTIR spectra of PAN and PAN/CNT fibers after stabilization.

Time/h	B_1				B_3				A_3			
	Φ_c/ %	Φ_b/ %	Φ_c/ Φ_b	Φ_d/ %	Φ_c/ %	Φ_b/ %	Φ_c/ Φ_b	Φ_d/ %	Φ_c/ %	Φ_b/ %	Φ_c/ Φ_b	Φ_d/ %
0.5	11.2	11.9	0.94	76.9	11	13.4	1.22	75	2.81	7.38	0.38	92.2
1	12.9	12.3	1.05	74.1	16.1	12.9	1.25	71	7.74	17.8	0.43	74.5
2	16.9	14.9	1.13	67.2	23.6	14.8	1.59	61.6	24.4	19	1.28	56.6
4	24.4	16.5	1.48	59.1	27	16.5	1.64	56.5	28.7	20.3	1.41	51

Note: Φ_c: Percentage of conjugated nitrile, Φ_b: Percentage of β-amino nitrile, Φ_d: Percentage of unreacted nitrile.

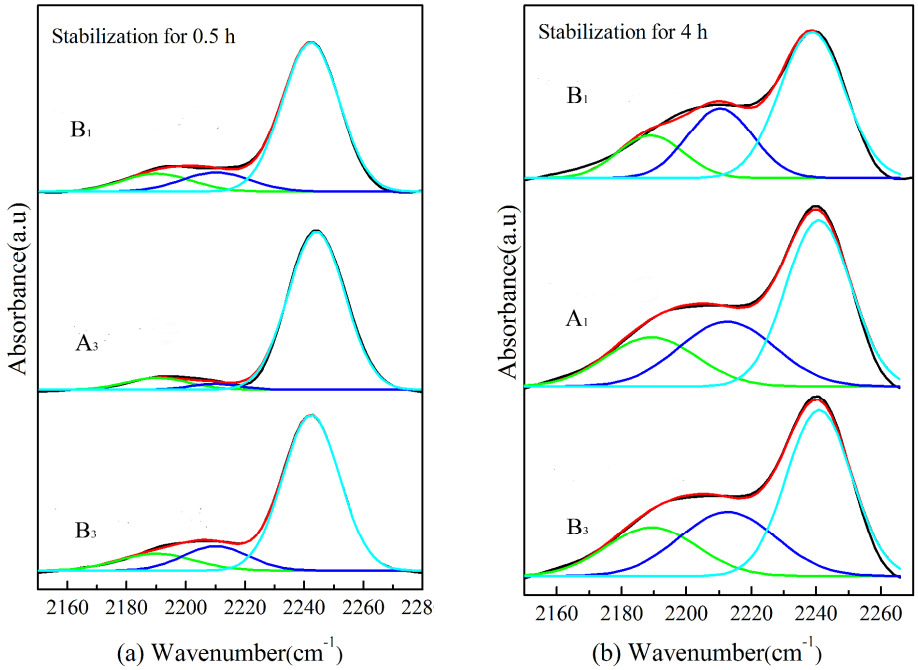

Fig. 9. Nitrile peak fitting of FTIR spectra of stabilized PAN and PAN /CNT composite fibers.

Table 5. Structural parameters of stabilized PAN and PAN/CNT composite fibers.

Time/ h	B_1		B_3		A_3	
	crystal size/nm	crystallinity /%	crystal size/nm	crystallinity/ %	crystal size/nm	crystallinity/%
0	1.44	51.8	1.63	60.3	1.38	58.6
0.5	1.19	50	1.2	56.7	1.2	58.1
1	1.13	49.7	1.14	54.6	1.15	57.3
2	1.12	49.5	1.12	49.7	1.11	47.4
4	1.08	48.3	1.1	48.2	0.99	43.1

Conclusion

In this paper, [Bmim]Cl was utilized as a plasticizer to achieve the plasticized spinning of PAN and PAN/CNT composite fibers. The interaction among the PAN, [Bmim]Cl and CNTs was investigated. For PAN/[Bmim]Cl/CNT system, it was revealed that the blue shift of C≡N groups induced by "cation-π" interaction is offset by red shift caused by "π-π"

interaction, thus the position of C≡N groups in the system is not shifted.

The tensile strength and modulus of PAN/CNT fibers were shown to increase with increasing draw ratio. The crystallinity was decreased at first, and then increased, which was associated with the oriented-crystallization rate and heat exchange rate. The planar zigzag conformation of the fibers exhibited an identical trend compared with crystallinity, revealing that the planar zigzag conformation was more likely to take place at amorphous region.

The initiation temperature for cyclization (T_i) of PAN fibers was increased with increasing draw ratio. This was because that the inter-molecular interaction became stronger with increasing draw ratio, which hindered the initiation of cyclization at amorphous region. However, the T_i of PAN/CNT fibers was decreased with increasing draw ratio. This was due to that the "π-π" interaction between PAN and CNTs and high draw ratio facilitated the intra-molecular cyclization at amorphous region. The introduction of CNTs contributed to the cyclization at amorphous region, but hindered the cyclization at crystalline region. For PAN/CNT fibers, drawing lowered the percentage of β-amino nitrile and accelerated the cyclization, which would improve the mechanical properties of resulting carbon fibers.

Acknowledgements

This work is supported by grants from the National High-tech Research and Development Projects (863, 2012AA03A605), the National Science Foundation of China (No. 51103019 and No. 21174027), Program for New Century Excellent Talents in University (No. NCET-12-0827), Program of Introducing Talents of Discipline to Universities (No. 111-2-04) .

Reference

[1] M. C. Paiva, C. A. Bernardo and M. Nardin, Carbon, 2000, 38, 1323.

[2] M. S. A. Rahaman, A. F. Ismail, A. Mustafa, Polym. Degrad. Stab., 2007, 92, 1421.
[3] J. Zhang, Y. W. Zhang, D. G. Zhang, J. X. Zhao, J. Appl. Polym. Sci., 2011, 125, E58.
[4] K. Sahin, N. A. Fasanella, I. Chasiotis, K. M. Lyons, B. A. Newcomb, M. G. Kamath, H. G. Chae and K. S. umar, Carbon, 2014, 77, 442.
[5] J. J. Ge, H. Q. Hou, Q. Li, M. J. Graham, A, Greiner, D. H. Reneker, F. W. Harris and S. Z. D. Cheng, J. Am. Chem. Soc., 2004, 126, 15754.
[6] H. L. Zhang, L. H. Xu, F. Y. Yang and L. Geng, Carbon, 2010, 48, 688.
[7] H. G. Chae, M. L. Minus, S. Kumar, Polymer, 2006, 47, 3494.
[8] P. Bajaj, T. V. Sreekumar and K. Sen, Polymer, 2001, 42, 1707.
[9] C. L. Lai, G. J. Zhong, Z. R. Yue, G. Chen, L. F. Zhang, A. Vakili, Y. Wang, L. Zhu, J. Liu and H. Fong, Polymer, 2011, 52, 519.
[10] M. C. Paiva, P. Kotasthane, D. D. Edie and A. A. Ogale, Carbon, 2005, 43, 1399.
[11] H. Zhou, X. Y. Tang, Y. M. Dong, L. F. Chen, L. T. Zhang, W. R. Wang and X. P. Xiong, J. Appl. Polym. Sci., 2011, 120, 1385.
[12] H. G. Chae, T. V. Sreekumar, T. Uchida and S. Kumar, Polymer, 2005, 46, 10925.
[13] H. G. Chae, Y. H. Choi, M. L. Minus and S. Kumar, Compos. Sci. Technol., 2009, 69, 406.
[14] Y. D. Liu, H. G. Chae and S. Kumar, Carbon, 2011, 49, 4477.
[15] Y. D. Liu, H. G. Chae and S. Kumar, Carbon, 2011, 48, 4466.
[16] Y. W. Ju, G. R. Choi, H. R. Jung and W. J. Lee, Electrochim Acta, 2008, 53, 5796.
[17] T. Maitra, S. Sharma, A. Srivastava, Y. K. Cho, M. Madou and A. Sharma, Carbon, 50, 1753.
[18] G. Wypych. Handbook of plasticizers. Toronto, Canada: ChemTech Publishing; 2004.
[19] L. Vaisman, E. Wachtel, H. D. Wagner and G. Marom, Polymer, 2007, 48, 6843.
[20] L, Vaisman, B. Larin, I. Davidi, E. Wachtel, G. Marom and D. W. Wagner, Composites: Part A, 2007, 38, 1354.
[21] M. Y. Wu, Q. Y. Wang, K. N. Li, Y. Q. Wu and H.Q. Liu, Polym. Degrad. Stab., 2012, 97, 1511.
[22] P. Rangarajan, J. Yang, V. Bhanu, D. Godshall, J. Mcgrath, G. Wilkes and D. J. Baird, J. Appl.Polym.Sci, 2001, 85, 69.
[23] C. L. Lai, G. J. Zhong, Z. R. Yue, G. Chen, L. F. Zhang, A. Vakili, Y. Wang, L. Zhu, J. Liu and H. Fong, Polymer, 2010, 52, 519.
[24] H. G. Chae, M. L. Minus, A. Rasheed and S. Kumar, Polymer, 2007, 48, 3781.
[25] C. L. Lai, G. J. Zhong, Z. R. Yue, G. Chen, L. F. Zhang, A. Vakili, Y. Wang, L. Zhu, J. Liu and H. Fong, Polymer, 2010, 52, 519.
[26] W. J. Wang, N. S. Murthy, H. G. Chae and S. Kumar, Polymer, 2008, 49, 2133.
[27] X. Li, A. W. Qin, X. Z. Zhao, B. M. Ma and C. J. He, Polymer, 2014, 55, 5773.
[28] V. B. Gupta and S. Kumar, J. Appl. Polym. Sci., 1981, 26, 1865.
[29] A. K. Gupta and R. P. Singhal, J. Polymer Sci. Polymer Phys.Ed., 1983, 21, 2243.
[30] T. Fukushima, A. Kosaka, Y. Ishimura, T. Yamamoto, T. Takigawa, N. Ishii and T. Aida, Science, 2003, 300, 2072.
[31] S. Bellayer, J. W. Gilman, N. Eidelman, S. Bourbigot, X. Flambard, D. M. Fox, H. C. De Long and P. C. Trulove, Adv. Funct. Mater., 2005, 15, 910.
[32] R. G. Peng, Y. Z. Wang, W. Tang, Y. K. Yang and X. L. Xie, Polymers, 2013, 5, 847.
[33] S. Rivera-Rubero and S. Baldelli, J. Phys. Chem. B, 2006, 110, 4756.
[34] Y. Jeon, J. Sung, D. Kim, C. Seo, H. Cheong, Y. Ouchi, R Ozawa and H. Hamaguchi, J. Phys. Chem. B, 2008, 112, 923.

[35] C. Cohen, G. B. Tanny and S. Prager, J. Polym. Sci. : Polym. Phys. Ed. 1979, 17, 477.
[36] S. Berber, Y. K. Kwon and D. Tomanek, Phys Rev Lett., 2000, 84, 4613.
[37] P. Kim, L. Shi, A. Majumdar and P. L. McEuen, Phys Rev Lett., 2001, 87, 215502-1.
[38] A. T. Chien, P. V. Gulgunje, H. G. Chae, A. S. Joshi, J. Moon, B. Feng, G. P. Peterson and S. Kumar, Polymer, 2013, 54, 6210.
[39] A. G. M. Ferreira, P. N. Simões, A. F. Ferreira, M. A. Fonseca, M. S. A Oliveira and A. S. M. Trino, J. Chem. Thermodyn., 2013, 64, 80.
[40] D. Sawai, A. Yamane, T. Kameda, T. Kanamoto, M. Ito, H. Yamazaki and Hisatani K, Macromolecules, 1999, 32, 5622.
[41] T. H. Ko, C. H. Lin and H. Y. Ting, J Appl Polym Sci, 1989, 37, 553-66.
[42] A. Gupta and I. R. Harrison, Carbon, 1996, 34, 1427.
[43] A. Gupta and I. R. Harrison, Carbon, 1997, 35, 809.
[44] S. B. Warner, D. R. Uhlmann and L. H. J. Peebles, J. Mater. Sci., 1979, 14, 1893.
[45] F. Lian, J. Liu, Z. K. Ma and J. Y. Liang, Carbon, 2012, 50, 488.
[46] Y. D. Liu, H. G. Chae and S. Kumar, Carbon, 2011,49, 4487.
[47] E. Fitzer, W. Frohs and M. Heine, Carbon, 1986, 24, 387.`
[48] H. S. Fochler, J. R. Mooney, L. E. Ball, R. D. Boyer and J. G. Grassell, Spectrochim Acta A, 1985, 41, 271.
[49] J. Liu, P. X. Zhou, L. F. Zhang, Z. K. Ma, J. Y. Liang and H. Fong, Carbon, 2009, 47, 1087.